

# Moonlighting Role of PEDF in Breast Cancer

**Carmen Gil-Gas**

UCLM: Universidad de Castilla-La Mancha

**Marta Sánchez-Díez**

UPM: Universidad Politecnica de Madrid

**Paloma Honrubia-Gómez**

UCLM: Universidad de Castilla-La Mancha

**Jose Luis Sánchez-Sánchez**

SESCAM: Servicio de Salud de Castilla-La Mancha

**Carmen Belen Alvarez-Simón**

SESCAM: Servicio de Salud de Castilla-La Mancha

**Sebastia Sabater**

SESCAM: Servicio de Salud de Castilla-La Mancha

**Francisco Sánchez Sánchez**

UCLM: Universidad de Castilla-La Mancha

**Maria del Carmen Ramírez Castillejo** (✉ [mariadelcarmen.ramirez@upm.es](mailto:mariadelcarmen.ramirez@upm.es))

Polytechnic University of Madrid: Universidad Politecnica de Madrid <https://orcid.org/0000-0002-1877-3381>

---

## Research article

**Keywords:** Breast cancer, Tumour initiating cells, PEDF, relapse, tumoral biomarkers, self-renewal

**Posted Date:** October 23rd, 2020

**DOI:** <https://doi.org/10.21203/rs.3.rs-93992/v1>

**License:** © ⓘ This work is licensed under a Creative Commons Attribution 4.0 International License.

[Read Full License](#)

---

## **Moonlighting role of PEDF in breast cancer**

Carmen Gil-Gas<sup>\*1</sup>, Marta Sánchez-Díez<sup>\*2</sup>, Paloma Honrubia-Gómez<sup>1</sup>, Jose Luis Sánchez-Sánchez<sup>3</sup>,  
Carmen Belen Alvarez-Simón<sup>1</sup>, Sebastia Sabater<sup>3</sup>, Francisco Sánchez Sánchez<sup>†1</sup>, Maria del Carmen  
Ramírez Castillejo<sup>†1,2</sup>

\* These authors contributed equally to this work. † These authors contributed equally to this work  
as Co-corresponding authors.

Affiliations: <sup>1</sup>University of Castile-La Mancha. <sup>2</sup>Technical University of Madrid. <sup>3</sup>Servicio de Salud  
de Castilla La Mancha.

Contact Information: [mariadelcarmen.ramirez@upm.es](mailto:mariadelcarmen.ramirez@upm.es) and [francisco.ssanchez@uclm.es](mailto:francisco.ssanchez@uclm.es)

1

### 2 **ABSTRACT**

3 Background: Breast cancer is the leading cause of death among females in developed  
4 countries. Although the implementation of screening tests and the development of new  
5 therapies has increased the probability of remission, relapse rates still remain high.  
6 Numerous studies have indicated the connection between cancer initiating cells and slow  
7 cellular cycle cells, identified by their capacity to retain long labelling (LT+).

8 Methods: We have designed a transgenic protein consisting in the C-terminal part of this  
9 protein, which acts by blocking endogenous PEDF in culture cell assays. Present work is  
10 based in doses-response in vitro assays as well as flow cytometry analysis of surface  
11 markers and cell cycle kinetic study of the tumour initiating cells.

12 Results: In this study we show that this type of cells is present not only in cancer cell lines  
13 but also in cancer cells from patients with metastatic and advanced stage tumours. We also  
14 present new assays showing how stem cell self-renewal modulating proteins, such as PEDF,  
15 can modify the properties, expression of markers, and carcinogenicity of cancer stem cells.

16 This protein has been involved in self-renewal in adult stem cells and has been described  
17 as anti-tumoral because of its anti-angiogenic effect. However, we show that PEDF  
18 enhances resistance in breast cancer patient cells *in vitro* culture by favoring a slow cellular  
19 cycle population (LT+). The PEDF signalling pathway could be a useful tool for controlling  
20 cancer stem cells self-renewal, and therefore control patient relapse.

21 Conclusions: We demonstrate that it is possible to interfere with the self-renewal capacity of  
22 cancer stem cells, induce anoikis *in vivo*, and reduce resistance against Docetaxel treatment  
23 in cancer patient cells *in vitro* culture. We have also demonstrated that this PEDF modified  
24 protein produces a significant decrease in cancer stem cell markers. All these properties  
25 make this protein a potential application in clinical cancer therapies via co-administration  
26 with chemotherapy for relapse cancer treatment.

## 27 **KEYWORDS**

28 Breast cancer, Tumour initiating cells, PEDF, relapse, tumoral biomarkers, self-renewal

## 29 **BACKGROUND**

30 The incidence of breast cancer has increased in recent years, due to an aging population[1].  
31 In fact, breast cancer is the leading cause of death among females in developed countries,  
32 although the implementation of screening tests and the development of anti-neoplastic  
33 therapies such as Trastuzumab has increased the probability of a cure in those patients[2].  
34 However, the relapse rate remains very high in different breast cancer types[3] and this is  
35 why further study of new pharmacological drugs and diagnostic methods is still needed.  
36 Relapse is mainly due to the tumour cell population's resistance, characterised by their  
37 capacity for self-renewal, resistance to drugs, and a slow cellular cycle[4,5]. This last  
38 characteristic allows for detection of this population, since this produces long retained  
39 labelling[6–8]. The auto-renewal capacity of these cells is essential for stem cells to be  
40 maintained throughout the life of the organism. Pigment Epithelium-Derived Factor (PEDF)

41 protein has been related to this self-renewal mechanism[9,10]. This protein may induce  
42 cellular differentiation and promote apoptosis in a variety of tumour cells[7,8], and it is also  
43 able to inhibit tumour proliferation, vascularization, cell migration, and metastasis[11–13]  
44 affecting the division of fast tumour cells. In addition, PEDF is a niche-derived regulator of  
45 adult neural stem cells [9,14,15] that activates slowly dividing cells without inducing  
46 proliferation nor differentiation [9,10]. Together with the fact that tumour initiating cells (TICs)  
47 within a tumor are capable of self-renewal, this is why this protein-signalling pathway could  
48 be important not only as an anti-neoplastic agent but also as a regulator of self-renewal in  
49 TICs and patient relapse. As has been widely described, PEDF is a pleiotropic molecule,  
50 presenting two domains with clearly differentiated functions, an anti-angiogenic part and a  
51 second domain with neurotrophic properties, each activating different signalling pathways.  
52 By using this fragmentation of the molecule into these two domains we are able to take  
53 advantage of their different effects on signalling pathways, including the carboxy-terminal  
54 fragment's inhibition of the crucial TICs population's self-renewal ability, which thus hinders  
55 tumour recurrence. This is why we suggest a new therapeutic mechanism that consists in  
56 the co-administration of carboxy-terminal PEDF protein fragments and chemotherapy.

57 In order to detect TICs, four different epitopes were analysed; these epitopes are implicated  
58 in the cells' different processes and have been previously related with cancer stem cells in  
59 literature. BCRP1 is a drug transporter from the ABC transporter family, but while it is not  
60 as ubiquitous as other family members, such as MDR1, it is commonly expressed in the  
61 population[16,17]. EpCAM is a transmembrane glycoprotein that is involved in cell signalling,  
62 migration, proliferation, and differentiation[18,19]. This whole process is closely related to  
63 the epithelial-mesenchymal transition, essential in the metastatic mechanism in which TICs  
64 could play an important role. CD133 is a pentaspan membrane glycoprotein that has been  
65 used as a stem cell biomarker since its discovery in 1999, although its function is still  
66 unknown. AC133 is a glycosylated-isoform of CD133, recognised by a specific antibody

67 which has been described as a biomarker for human hematopoietic stem cells and different  
68 cancer stem cell models[20–23].

69 All these proteins have been involved in different metastatic processes, and could be a  
70 target for new therapies but, more interestingly, they can be indicators of the process'  
71 progress and could suggest what the mechanism and the signalling pathway of these cells  
72 involved in the resistance to chemotherapeutic treatments is. One of the cellular  
73 mechanisms that may be involved in these resistance processes is anoikis[24–28]. Anoikis  
74 is a form of apoptosis that occurs in anchorage-dependent cells and in a niche context, when  
75 the cells detach from the surrounding extracellular matrix (ECM) and lose the connection to  
76 the nurse surrounding cells[28,29]; this is one of the processes we observed after the  
77 combination of chemotherapy and treatment with the carboxy-terminal part of PEDF protein.

78 In this scenario, we have addressed the problem of locating breast tumour-initiating cells,  
79 and the study of the self-renewal mechanism by inhibiting its functionality and potential  
80 tumour recurrence. We also postulate that the PEDF signalling pathway could be a potential  
81 therapeutic target for control of cancer initiating cells' self-renewal and tumour relapse, as  
82 has been postulated in other neoplastic models[30].

## 83 **MATERIALS AND METHODS**

### 84 **CELL CULTURE**

85 MCF7 (ATCC® HTB-22™), MDA-MB-231 (ATCC® HTB-26™) and 293 HEK-293 (ATCC®  
86 CRL-1573™) cell lines were acquire from ATCC company (Manassas, Virginia, United  
87 States). Pa00 was derived in the laboratory from metastatic patient pleural effusion[31].  
88 Pa00, MCF7 and MDA-MB-231 cells were maintained in DMEM (Lonza. Basel, Switzerland)  
89 10% FBS (Lonza), 1% Glutamine (Lonza) (0,2M) and 1% Penicillin/streptomycin (Lonza)  
90 (100 units+100 ug/10ul) in a 5% CO<sub>2</sub> humidified incubator at 37°C.

### 91 **STAIN WITH DDAO AND SORTING**

92 Cells for cell cycle dynamic assays were plated (100 000 cells). Next, these cells were  
93 washed with PBS, disaggregated and then incubated at 37°C with Cell Trace ® Far-Red-  
94 DDAO-SE (DDAO-SE, Molecular probe ref C34564. Eugene, Oregon, United States), at the  
95 concentration recommended in the product data sheet. After 10 min, an aliquot of freshly  
96 labeled cells (approx. 200 000 cells) was fixed with 0,5% of paraformaldehyde to use as a  
97 positive control for the experiment. Then, cells were centrifuged at 180g for five minutes and  
98 suspended in the culture medium to grow under standard conditions. Eight days *in vitro* later,  
99 cells were disaggregated and sorted by In-flux™ (Becton Dickinson. Franklin Lakes, New  
100 Jersey, United States) sorting equipment depending on their fluorescent retaining labeling  
101 level. Positive cells were considered slowly dividing cells, and thus potential tumour initiating  
102 cells.

### 103 CYTOMETRY ASSAY

104 Cytometry assays were performed with a MACSQuant Analyzer 10 cytometer (Miltenyi  
105 Biotec ref 130-096-343. Bergisch Gladbach, Germany). Samples were first washed in PBS  
106 and incubated with Miltenyi Biotec FcR blocking Reagent (human), in 100 microliters of  
107 sample. The immunostaining was performed per the standard protocol recommended by  
108 the commercial houses of the different antibodies. The antibodies and the working  
109 dilutions used were as follows: AntiBCRP-FITC 5D3 Chemicon (Temecula, California,  
110 United States) and AntiBCRP-PE 5D3 Chemicon incubated for 20 minutes at a 1:10  
111 dilution; while AntiEpCAM- PE Clon HEA-125, AntiAC133-PE Clon AC133, AntiCD133-PE  
112 293C3, Anti CD44-FITC and CD24-PE, all from Miltenyi Biotec, were incubated 10 minutes  
113 at a 1:11 dilution. Sorting experiments were performed with a BD Influx™ cell sorter. FITC  
114 or PE are used as abbreviation of Fluorescein isothiocyanate and Phycoerythrin  
115 respectively.

### 116 XENOGRAFTS

117 FOXn1nu females, at 1 month of age were obtained from Charles River International  
118 Laboratories (Wilmington, Massachusetts, United States) to use in these experiments.  
119 Animals were housed and bred under 20-25 °C, humidity of 50-60% and a 12 hours' light-  
120 dark cycle. All experiments were performed in accordance with relevant guidelines and  
121 regulations and the animals were treated in accordance with the approval of the local ethics  
122 committee (University of Castilla-La Mancha PI081746). The experiments were performed  
123 as previously laboratory assays[30]. In sort, untreated cells (control) and treated cells (8nM  
124 CTE-PEDF) suspended in PBS were injected subcutaneously on both flanks of those  
125 immunocompromised mice. 5 000 cells were injected in a final volume of 200 uL 1:1 dilution  
126 Matrigel™ Basement Membrane Matrix (Becton Dickinson) with a 25 gauge-needle. Tumour  
127 growth was monitored weekly with a caliper. The final tumour volume was calculated as  $V =$   
128  $2 \times L_1 \times L_2 \times \pi/6$ . Tumours were mechanically and chemically dissociated with collagenase  
129 and trypsin at 37°C. They were then washed with PBS and seeded in DMEM medium, 10%  
130 FBS, 1% glutamine (200 mM), 1% Penicillin/streptomycin, 0.5% EGF and 0.04% FGF in a  
131 5% CO<sub>2</sub> humidified incubator at 37°C 12h before start the rest of the experiments.

## 132 PEDF and CTE-PEDF PRODUCTION

133 PEDF and Cter-PEDF were cloned into pcDNA™3.1/myc-His A, B, & C Mammalian  
134 Expression Vectors (Invitrogen™. Carlsbad, California, United States) following the protocol  
135 previously described by [32]. After cloning, vectors were checked by sequencing (3130  
136 Applied Biosystems. Foster City, California, United States). Serine 227 was mutated into a  
137 glutamate (E) residue using *ser227glu-dw* (5'-CCA AGT AGA AAT CCT CGA GCT CAG  
138 TCT TTC TGG AGT-3') and *ser227glu-up* (5-GTT TGA CTC CAG AAA GAC TGA GCT CGA  
139 GGA TTT CTA-3) primers. Proteins were produced by HEK-293-T cells after transfecting  
140 with phosphate calcium. Conditioned mediums were collected after 3 DIV, quantified by  
141 western-blot using anti-c-myc mouse monoclonal IgG1 (Santa Cruz Biotechnology. Dallas,  
142 Texas, United States), and anti-phosphoserine clone 4A4, (Millipore. Burlington,

143 Massachusetts, United States) and stored at -20°C or purified using GE Healthcare Life  
144 Sciences™ HisTrap™ FF Crude columns (Thermo Fisher Scientific, Waltham,  
145 Massachusetts, United States).

#### 146 TREATMENT WITH PEDF AND CTE-PEDF

147 Cells were treated with PEDF or CTE-PEDF at a final concentration of 8 nM in the medium.  
148 The acute treatment consists of a single treatment: two hours of peptide exposure before  
149 chemotherapy treatment. Chronic treatment consists of six peptide treatments (culture  
150 medium with CTE once per week), totalling six weeks of peptide exposure before  
151 chemotherapy treatment.

#### 152 DOSE-RESPONSE CURVE

153 Cells were plated in a 24-well plate at a final concentration of 15 000 cells/well in a total  
154 volume of 200 microliters or 200 cells/well in a 96-well plate for sorted cells. Half of the plate  
155 was plated with CTE-PEDF medium. The next day, the drug was added in increasing  
156 concentrations 4 nM, 2 nM, 1 nM, 0.5 nM, 0.25 nM. These were cultured for 3 days under  
157 drug exposure in *in vitro* conditions, and then developed with an MTT assay or methyl purple  
158 assay.

#### 159 MTT ASSAY

160 Supernatant was removed, after which 100 microliters/well of 3-(4,5-dimethylthiazol-2-yl)-  
161 2,5-diphenyltetrazolium bromide ( ) was added. After 30 minutes of incubation, the  
162 supernatant was again removed, and the precipitated crystals were dissolved in 100  
163 microliters of DMSO. The plate was read in a spectrophotometer at 540 nm.

#### 164 METHYL PURPLE ASSAY

165 This method[30] is used to quantify surviving cells. 5 000 cells/well were seeded in 24-well  
166 plates, in a final volume of 250 µL. The next day, cells were treated with increasing doses

167 of chemotherapeutic agents and stored in a humidified incubator at 37°C, 5% CO<sub>2</sub> for 4 days.  
168 Then, cells were fixed with 0.5% glutaraldehyde (Sigma. St. Louis, Missouri, United States)  
169 for 10 minutes. Next, cells were stained with 0.1% crystal violet for 20 minutes. After several  
170 washes with PBS, 10% acetic acid was used to solubilize the sample. Finally, a  
171 spectrophotometric reading was performed at a wavelength of 590 nm. IC<sub>50</sub> value was  
172 determined as the dose of drug necessary to eliminate 50% of the cell population, obtained  
173 through logarithmic regressions made with the DE.0 plus v 1.0 program.

#### 174 HISTOLOGY

175 Cryostat sectioning slides were performed using a cryostat (Microm HM 550, Thermo  
176 Scientific). Tumour samples were fixed with formaldehyde at 4%, placed in sucrose 30%  
177 overnight, included into Tissue-Tek® OCT™ (Sakura ® Finetek USA. Torrance, California,  
178 United States) and then frozen with liquid nitrogen. Slides (12µm) were stained with  
179 hematoxylin and mounted with Dako Ultramount Aqueous Permanent Mounting Medium  
180 (Agilent Technologies. Santa Clara, California, United States) and analyzed with a Leica-  
181 DMRXA-photomicroscope (Leica. Wetzlar, Germany).

#### 182 ANALYSIS OF CELL MORPHOLOGY

183 500 000 treated and control cells were seeded in p100 plates. After 24 hours, cells were  
184 incubated for 30 minutes with Hoechst (5µg/mL). Ten random microscopy images were  
185 taken (Motic AE31. Barcelona, Spain) using an ultraviolet light. Analysis of the cytoplasmic  
186 area and the separation between cells was analyzed using the Image J application  
187 (<https://imagej.nih.gov/ij/>).

#### 188 STATISTICAL ANALYSIS

189 Data was analyzed with R software 3.5.1 version (<https://www.r-project.org/>). The statistical  
190 analysis was carried out using Mann-Whitney U tests (one tailed, significance level=0.05).  
191 The data is expressed as the mean plus the standard error (SE). At least n=3 independent

192 experiments were performed for every assay. The results obtained are considered  
193 statistically significant when  $p < 0.05$  (\*),  $p < 0.01$  (\*\*) and  $p < 0.005$  (\*\*\*). Blood cell data was first  
194 transformed into a quadratic variable to improve data homogeneity. Then, normality was  
195 tested using the Shapiro-Wilk test, Q-Q plots, and Levene's test for homogeneity of variance.  
196 Next, groups were compared using non-parametrical Kruskal-Wallis test by ranks and  
197 Wilcoxon's not paired test to analyse data in pairs. Finally, logistic regression was used to  
198 model the relationship between the number of cells and progression. The odds ratio was  
199 used to strengthen the association between variables (Confidence Interval 95%).

## 200 RESULTS

### 201 1. Long retaining labelling cells exhibit characteristics of cancer stem cells, in 202 cancer cell lines and in cancer patient cells.

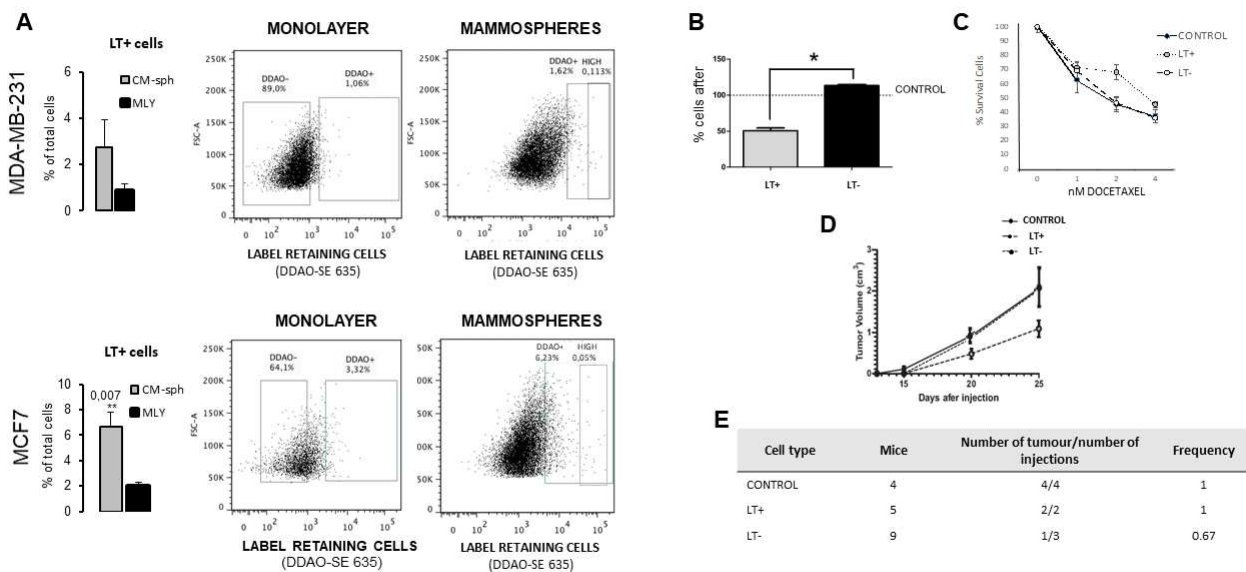
203 MDA-MB-231 and MCF7 breast adenocarcinoma cell lines exhibit a cell population  
204 characterized by long retained labelling growing either in adherent or mammosphere  
205 conditions (Figure 1A). A population of  $0.9 \pm 0.3$  % and  $3 \pm 1$ % of long retaining labelling  
206 cells is present when the MDA-MB-231 cell line is grown in an adherent monolayer and in  
207 mammosphere conditions, respectively. In mammosphere conditions, it is possible to see  
208 0.1% of total cells with high labelling. This result is also seen for the MCF7 cell line where  
209 the percentage of long labelling cells is 3.32% and 6.28% (0.5% high labelled) in monolayer  
210 culture and mammosphere conditions, respectively.

211 Ascitic fluid cells from a patient with a metastatic adenocarcinoma (Pa00 cells) also  
212 present long retaining labelling cells after 8 days in culture. A methyl purple assay proves  
213 that LT- cells show the same growth rate as our control cells but have a higher growth rate  
214 than LT+ cells (Figure 1B). Those cells underwent a dose-response assay with Docetaxel  
215 chemotherapy. As we can see in Figure 1C, even though LT+ cells grow less than LT- or  
216 control cells, they are more resistant to chemotherapy than control or LT- cells (IC50 value  
217 is double in the case of LT+ cells compared to control or LT- cells). Docetaxel treatment  
218 eradicates 53% of LT- cells at 2 nM, while only 27% of LT+ were affected by the same  
219 concentration.

220 Finally, Pa00 LT+ and LT- sorted cells were injected in nude mice to study the  
221 carcinogenicity of those populations in vivo. This experiment shows that the tumour volume  
222 is similar when injecting LT- cells and control non-separated cells but smaller when injecting  
223 LT+ cells (Figure 1D). In addition, Pa00 LT- cells failed to form tumours after cell injection.

224 That's why the frequency of tumour formation is lower when injecting LT- cells than LT+  
 225 cells or control non-separated cells (Figure 1E).

226 In short, LT+ cells show a lower growth rate and are more resistant to chemotherapy  
 227 than LT- or control non-separated cells. In addition, *in vivo* assays reveal a decrease in the  
 228 frequency of tumour formation in LT- cells when compared to LT+ or control cells.



229 **Figure 1. LT+ population display cancer stem cells characteristics.** (A) Cells were  
 230 stained with DDAO and cultivated 8DIV in monolayer or as mammospheres. Both cell  
 231 lines showed LT+ population and it was higher in mammosphere assays (cytometry  
 232 assay). Quantification of LT+ cells (n=3) is shown. (B) Growing patterns of LT+ and  
 233 LT- cells. Pa00 cells were stained, grown 8DIV (400cells/well) and then sorted  
 234 according to their DDAO content. It was checked the number of living cells after 3DIV  
 235 by methyl purple assay. LT- cells grew similar to control and faster than LT+ cells. (C)  
 236 Docetaxel dose-response curves for LT+, LT- and control cells. Cells were stained  
 237 with DDAO and grown for 8DIV, sorted by their content of DDAO and grown with  
 238 increasing concentration of docetaxel. LT+ cells showed more resistance against  
 239 docetaxel than LT-.

(D) 5000 cells were injected in nude mice in each case. The

240 volume of the tumour is similar when injecting LT- cells and control non-separated  
241 cells but smaller when injecting LT+ cells. All tumours were palpable at the same time.  
242 LT+ tumours grew slowly compared to control or LT- group. (E) Pa00 LT- cells failed  
243 to form tumours when injected in a small amount of cells. All set of tumour cells were  
244 able to form tumours when 5000 cells were injected. However, LT- cells displayed a  
245 less frequency in tumour forming when 1200 or 350.000 cells were injected.

246 **2. PEDF modulate CSC properties, producing an increase of drug resistance**  
247 **and increasing LT+ cells proportion.**

248 PEDF is a verified modulator of stem cell self-renewal[14,33]. PEDF chronic  
249 treatment produces morphological changes in size and cytoplasm shape of Pa00 cells in  
250 culture (Figure 2A). An increment of  $170 \mu\text{m}^2$  of the cytoplasmic area is shown in PEDF  
251 treated cells ( $730 \pm 80 \mu\text{m}^2$  in PEDF treated and  $560 \pm 30 \mu\text{m}^2$  in control medium). However,  
252 there are no significant differences between the nucleus size with and without treatment  
253 (Figure 2B).

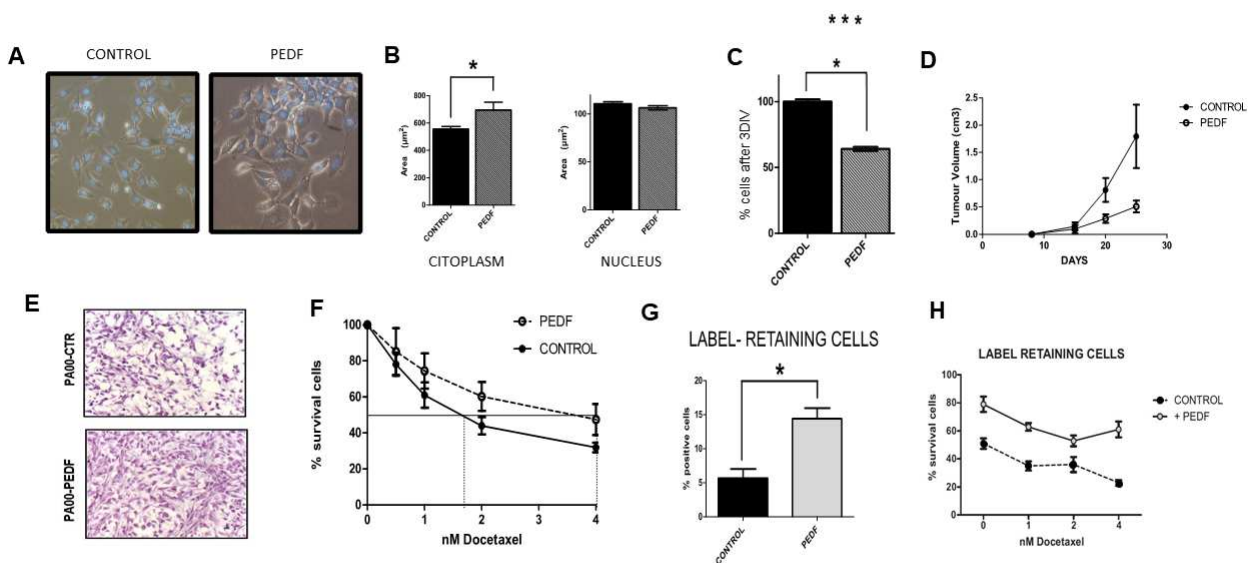
254 We have also studied the growing pattern of chronically PEDF-treated patient cells.  
255 Close to a 40% decrease in cell growth can be seen in treated cells compared to controls  
256 (Figure 2C). This slower growth rate of treated cells translates into a lower tumour volume  
257 and less necrotic area when comparing with control untreated cells. The histological analysis  
258 of the xenograft, showed that PEDF treated tumours present smaller necrotic areas than  
259 control xenografts. PEDF treatment also produces a compact growth of the tumoral cells  
260 with dense cytoplasm and compact external matrix compared to control tumours (Figure 2D-  
261 E).

262 These cells were also checked in a dose-response assay, and despite their low  
263 growth rate, PEDF treated cells exhibit higher IC50 values and resistant population, as 47%  
264 of PEDF treated cells survived, which means there were 16% more resistant cells than in

265 the control. This result implies a higher drug resistance to Docetaxel than control cells  
 266 (Figure 2F).

267 We carried out the next assay to prove that the slow growth observed *in vitro* and *in*  
 268 *vivo* is due to the appearance of a higher number of slow-cycle cells after PEDF treatment.  
 269 The quantification of LT+ cells after 3DIV revealed a significant increase after PEDF  
 270 treatment compared to the control (Figure 2G). A dose-response assay was performed, and  
 271 the results demonstrate that the resistance to docetaxel is 38% higher in PEDF treated cells  
 272 at 4 nM than in the control group (Figure 2H).

273 To sum up, PEDF treated cells show changes in the cytoplasm size, a decrease of cell  
 274 cycle kinetics, an increase in drug resistance, and the capacity to produce tumours with not  
 275 only a lower growth rate but also lower tumour volume and fewer necrotic areas.



276 **Fig 2. Pigmental Epithelium Derived Factor (PEDF) increases the number of LT+ cells**  
 277 **and the Docetaxel resistance of breast cancer cells.** (A) Cells treated with chronic  
 278 PEDF showed a different morphology than control. (B) Quantification of morphology  
 279 differences induced by PEDF treatment. (C) Growing pattern n=3 after 3DIV of PEDF  
 280 treated cells and control. PEDF chronic treated cells grew slower than control. (D)

281 Docetaxel dose-response curve of PEDF treated cells and control, n=3. PEDF chronic  
282 treated cells were more resistant against Docetaxel. (E) PEDF chronic treatment  
283 increased the number of LT+ cells in vitro (n=3). (F) Docetaxel dose-response curve  
284 of LT+ PEDF treated cells and LT+ cells, n=3. LT+ PEDF chronic treated cells were  
285 more resistant against Docetaxel than LT+. (G) PEDF treated cells and control cells  
286 were injected into nude mice. PEDF chronic treated cells grew slower than control. (H)  
287 Histology of PEDF treated tumours and control tumours. Necrotic areas are bigger in  
288 control compared to PEDF treatment.

289

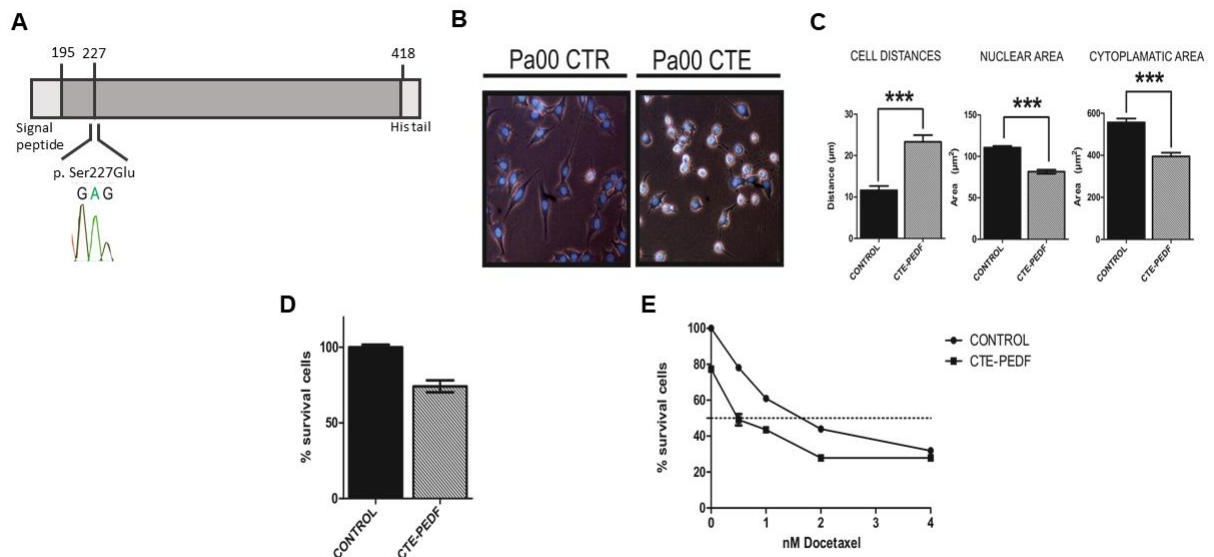
290 **3. Cter-PEDF counteracts the effects of native PEDF, decreasing the resistance**  
291 **in tumours and inducing anoikis and depleting CSC.**

292 As the truncated protein CTE-PEDF does not exhibit the same effects in stem cells as  
293 the full-size PEDF protein, we decided to check if this peptide would counteract the  
294 effects of the native protein. This protein presents phosphorylation sites that are  
295 important for the protein's function. In order to maintain the negative charge, a glutamate  
296 was introduced in position 227 of the protein's sequence, where a serine was previously  
297 located. This modification leads to the CTE-PEDF protein (Figure 3A). In vitro treatment  
298 with CTE-PEDF (200ng/ml) was performed in patient cultured cells. This experiment  
299 shows an anoikis effect (Figure 3B) and morphological changes that can be measured  
300 by cytoplasmic and nuclear areas and cell distances (Figure 3C). Nuclear and  
301 cytoplasmic areas are reduced 29% (Nuclear area: control  $110 \pm 2 \mu\text{m}^2$ , CTE  $81 \pm 2.34$ ;  
302 Cytoplasmic area control:  $556 \pm 18 \mu\text{m}^2$ , CTE:  $394 \pm 17 \mu\text{m}^2$ ) while cell distances double  
303 their size (control  $12 \pm 1 \mu\text{m}^2$ , CTE:  $23.0 \pm 0.2 \mu\text{m}^2$ ).

304 The next approach was a dose-response assay with Docetaxel. The result  
305 demonstrates that CTE-PEDF treated cells are less resistant to the drug than control  
306 cells. Just the CTE-PEDF treatment produces a 20% reduction of the initial population

307 (Figure 3D). The IC50 value is double in the control group when compared to CTE-PEDF  
 308 treated cells (Figure 3E).

309 The results demonstrate that CTE-PEDF produces anoikis in cancer patient cells and  
 310 reduces the drug resistance to Docetaxel.

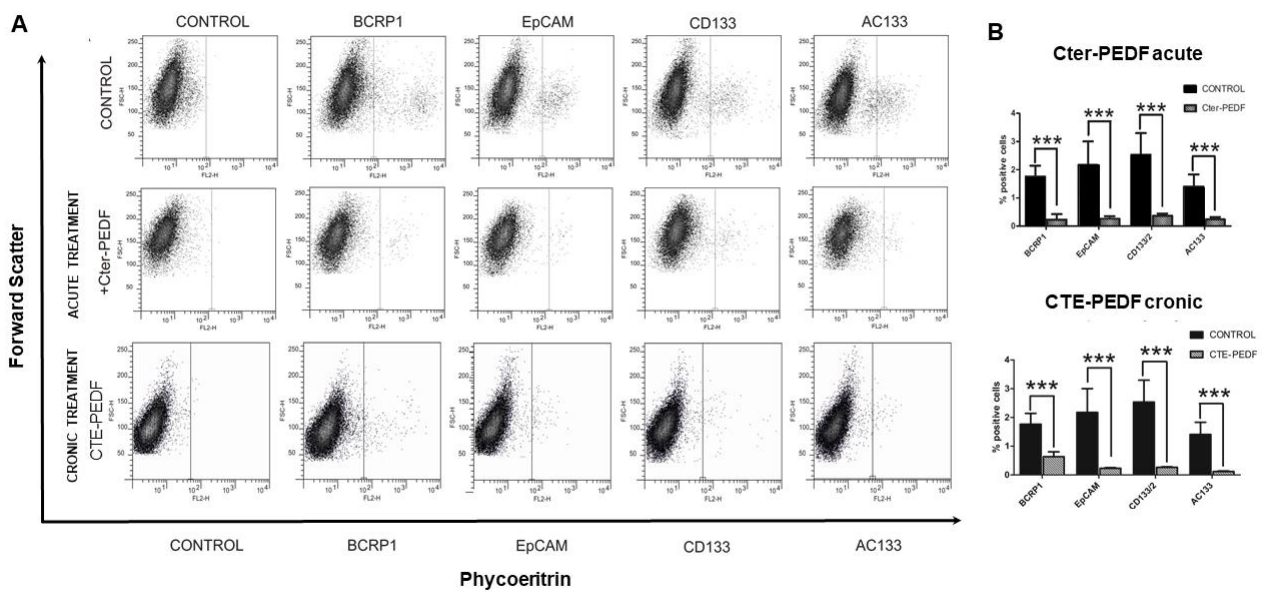


311 **Fig 3. CTE-PEDF induces anoikis in vivo and reduces resistance against Docetaxel**  
 312 **without affecting LT+ population.** (A) CTE-PEDF construction (B) Pa00 cells were  
 313 treated chronically with CTE (200ng/uL). After a week they showed an increase in  
 314 anoikis. (C) Quantification of CTE induced morphology. (D) Growing pattern n=3 after  
 315 3DIV of CTE treated cells and control. CTE chronic treated cells grew slower than  
 316 control. (E) Docetaxel dose-response curve of CTE treated cells and control, n=3.  
 317 CTE chronic treated cells were less resistant against Docetaxel.

318 **4. CTE-PEDF depletes CSC expression markers.**

319 We already know the effect produced in cells decreasing their resistance and  
 320 inducing anoikis as is show in previos results, when cultures are treated with CTE-PEDF  
 321 but, what we are now considering is whether this effect is produced because of a  
 322 reduction in CSC number and thus, in CSC expression markers. To solve this question,

323 Pa00 cells were injected with CTE-PEDF or PBS in nude mice. Tumours were dissected  
 324 and dissociated to study stemness marker expression by flow cytometry. Four different  
 325 epitopes, that have been previously related with cancer stem cells, were analysed:  
 326 BCRP1, EpCam, CD133 and AC133. CTE-PEDF treatment produces a significant  
 327 reduction in all studied markers in patient tumour cells Pa00. The same experiment was  
 328 performed with cells chronically treated in culture with CTE-PEDF, and the same  
 329 reduction in marker expression was observed (Figure 4).



330 **Fig 4. Cter-PEDF and CTE-PEDF treatments decrease CSC in vivo in Pa00 ascitis cell**  
 331 **line.** (A) 5000 Pa00 cells were injected in matrigel with 200ng/uL of Cter-PEDF, CTE-  
 332 PEDF or PBS (control). A cytometry assay showed that the number of CSC is lower  
 333 in both treatments compared to control. (B) Quantification of positive cells in each  
 334 treatment compared to control (n=3). Significant differences are shown.

335  
 336 In conclusion, CTE-PEDF decreases putative stemness markers involved in self-  
 337 renewal and patient release. They could be interesting proteins to control drug-resistant  
 338 cells populations in patient samples.

339 **DISCUSSION**

340 Breast cancer is the most common cancer in women worldwide. We study how to prevent  
341 relapse, taking breast cancer as an example because of its impact on the population. It's  
342 important to distinguish tumour initiating cells, responsible for tumour formation, and also  
343 probably for tumour relapse, and this is why we have focused on marker expression to detect  
344 this kind of cells (TICs). A combination of different epitopes found in the literature was  
345 applied to detect these cells[34–36]. Later, our objective was to discover a possible new  
346 treatment for patients in which TICs were detected. We demonstrate that PEDF (and  
347 derivatives) have a moonlighting role in breast cancer development and relapse, and it has  
348 a potential application in clinical cancer therapies by the co-administration with  
349 chemotherapy for relapse cancer treatment. This is the case of CTE-PEDF, that decreases  
350 drug resistance[37,38]. The co-administration with chemotherapy would lead to a less  
351 resistant population because TICs would have changed and lost their stemness  
352 characteristics, as we discuss in the following sections.

353 **About the stemness characteristics of long retaining labelling cells, in cancer**  
354 **cell lines and in cancer patient cells.**

355 We have shown that MDA-MB-231 and MCF7 breast adenocarcinoma cell lines  
356 exhibit a cell population characterized by long retained labelling growing either in adherent  
357 or mammosphere conditions, as has been previously described in other tumour cell  
358 lines[39–41]. Other researchers have detected a similar percentage of stemness and  
359 invasiveness for breast cancer cells in these cell lines, which was modified by oestrogen  
360 through Gli1 activation[42]. Even in mammosphere cultures, we have observed that a high  
361 DDAO positive population remains after 8 days in culture. These cells, with slow kinetic cell  
362 division, have probably only divided once in this period. This subpopulation could be related  
363 to the resistant cells maintained by IL-6 in some breast cancer treatments, such as the  
364 inhibitor of the human epidermal growth factor receptor 2 (HER2) Lapatinib [43].

365 Ascitic fluid cells from a patient with a metastatic adenocarcinoma (Pa00 cells) have  
366 been used in this paper parallel to the use breast cancer cell lines. Ascitic fluid should be an  
367 acellular liquid resulting from inflammation events. After metastasis progression, ascitic fluid  
368 could contain tumour cells that grow in culture conditions[44,45]. These cells also present  
369 long retained labelling after 8 days in culture, so we sorted these cells according to their  
370 DDAO content. This experiment showed that LT+ cells grow more slowly than LT- cells and  
371 respond less to chemotherapy than control or LT- cells. We postulated that this is the reason  
372 for the resistance observed in some treatments. Similar differences in resistance have also  
373 been observed in other colon and breast cancer cell lines[6] and even in other more  
374 aggressive type of tumours as a glioblastoma C6 cell line[37]. The final percentage of  
375 resistant cells after maximum physiological doses of Docetaxel treatment is also higher in  
376 LT+ positive cells than in the rest. This LT+ population that supports higher Docetaxel IC50  
377 than LT- or control cells could be the origin of patient relapse and related to a higher BCRP1  
378 and CD133 marker expression. To investigate this hypothesis, Pa00 LT+ and LT- sorted  
379 cells were injected in nude mice to study the tumorigenicity of those populations. We have  
380 considered not only the final volume of the xenograft tumours, but also the timing of the  
381 tumours' appearance. LT- cells formed tumours at the same time as control non-separated  
382 samples but LT+ Pa00 cells, which have a decrease in the kinetic division of their cell cycle,  
383 took longer to form tumours. Accordingly, the percentage of final tumour growth after LT+  
384 cell injection is 1/3 higher than in LT- xenografts. This result, together with the previously  
385 shown data, leads us to consider that the difference between these two cell types is the  
386 initial tumour capacity. This data correlates with previous data from research groups that  
387 correlate chemoresistance, tumorigenicity potential, and slow-cycling in some tumour  
388 cells[39–41].

389 All this data supports the hypothesis that LT+ cells present slow cell cycle division, higher  
390 chemotherapy resistance, and higher frequency of tumour formation than LT- or control cells.

391 These characteristics confirm the idea that LT+ cells could be involved in relapse and  
392 metastasis progression in breast cancer.

393 **PEDF modulates tumour initiating cells and causes an increase of drug**  
394 **resistance and LT+ population.**

395 PEDF chronic treatment produces a decrease in the growth rate *in vitro* and *in vivo*  
396 due to an increase in the number of LT+ cells (slow-cycle cells). Despite their low growth  
397 rate, PEDF treated cells show higher IC50 value and resistant populations than control,  
398 indicating higher resistance to chemotherapy. One possible explanation for this effect could  
399 be that the low growth rate leads to more time for these cells to repair chemotherapy damage,  
400 even though another hypothesis could contribute to this stage, such as higher expression of  
401 ABC drug transporters in these cells.

402 **CTE-PEDF counteracts the effect of native PEDF and depletes TICs markers**  
403 **expression**

404 As we have shown here, CTE-PEDF treated patient cells showed anoikis and  
405 morphological changes in culture. What is known as the anoikis effect is the apoptosis  
406 induced by the lost, insufficient, or inappropriate interactions between the cell and the  
407 extracellular matrix[46]. This effect could be the base for the interaction of TICs with the  
408 surrounding niche, and could be involved in the loss of stemness properties and  
409 chemotherapy resistance. Docetaxel resistance decreases when cells are treated with  
410 CTE-PEDF. It counteracts the effect of PEDF, which is a niche protein[9] involved in self-  
411 renewal and trophic maintenance of pluripotent cells. PEDF is secreted by endothelial  
412 cells and is one of the proteins involved in the self-renewal stem cell capacity. Endothelial  
413 cells also play a significant role in tumour progression and metastasis[47], and the niche  
414 signals could be key to understanding tumour progression, epithelial-mesenchymal  
415 transition, and distant metastasis at patient relapse. A significant difference is shown

416 between treated cells and controls, with PEDF or derived peptides, but the protocol  
417 followed in this experiment should be standardized to obtain a better result. The  
418 resistance of these cells is because they come from a patient in advanced metastasis  
419 ascites.

420 Expression of markers that had been previously related to cancer stem cells  
421 decreases when cells are treated with CTE-PEDF. This effect confirms the idea that  
422 CTE-PEDF produces a decrease in resistance to drugs such as Docetaxel, because it  
423 reduces the number of tumour initiating cells. That indicates a possible potent application  
424 as a future treatment for this protein when co-administered with chemotherapy. Although  
425 further studies need to be carried out, these experiments point to a possible new strategy  
426 for relapse cancer treatment.

## 427 **CONCLUSIONS**

428 The PEDF stem cell self-renewal modulator protein modify the carcinogenicity of cancer  
429 stem cells and could be a useful tool to control its self-renewal and therefore control patient  
430 relapse. We have designed a transgenic peptide derived from PEDF to interfere with the  
431 self-renewal capacity of cancer stem cells, inducing anoikis in vivo and reducing resistance  
432 in cells from cancer patients. We have also shown that this PEDF-derived protein produces  
433 a significant decrease in cancer stem cell markers, making this protein a potential tool for  
434 delaying patient relapse.

## 435 **LIST OF ABBREVIATIONS**

436 LT+: retain long labelling

437 PEDF: Pigment Epithelium-Derived Factor

438 TICs: tumour initiating cells

439 ECM: extracellular matrix

440 HER2: epidermal growth factor receptor 2

441 **DECLARATIONS**

- 442 • Ethics approval and consent to participate: The Ethics Committee of the “Complejo  
443 Hospitalario de Albacete” gave its approval for the present study to be carried out  
444 with the corresponding informed consents.
- 445 • Consent for publication: All authors give our consent for the publication of the data  
446 reflected in this article.
- 447 • Availability of data and materials: All data and materials are described in the  
448 corresponding sections of this article. There is no supplementary material.

449 **CONFLICTS OF INTEREST:** The authors declare no competing financial and non-  
450 financial interests in relation to the work described.

451 **FUNDING:** Research Project from the “Asociacion Española Contra el Cancer”,  
452 Albacete Regional Division. Programa Propio Universidad Politécnica de Madrid.

453 **AUTHOR CONTRIBUTION STATEMENT:** 1. Conception or design of the work:  
454 Carmen Ramírez-Castillejo; Francisco Sánchez-Sánchez 2. Data collection. Carmen  
455 Gil Gas; Paloma Honrubia Gómez; Carmen Belén Alvarez-Simón; Jose Luis Sánchez;  
456 Sebastián Sabater. 3. Data analysis and interpretation. Carmen Ramírez-Castillejo;  
457 Carmen Gil Gas; Francisco Sánchez-Sánchez; Marta Sánchez-Díez. 4. Drafting the  
458 article. Carmen Gil Gas; Marta Sánchez-Díez; Francisco Sánchez-Sánchez 5. Critical  
459 revision of the article. Carmen Ramírez-Castillejo; Carmen Gil Gas; Francisco Sá  
460 nchez-Sánchez; Marta Sánchez-Díez, Paloma Honrubia-Gómez, Jose Luis Sánchez,  
461 Sebastián Sabater. 6. Final approval of the version to be published. Carmen Ramírez-

462 Castillejo; Francisco Sánchez-Sánchez; Marta Sánchez-Díez, Paloma Honrubia-Gó  
463 mez, Jose Luis Sánchez, Sebastián Sabater.

#### 464 **ACKNOWLEDGMENTS:**

465 We thank C.E. Gavira O Neill for reading the manuscript and English correction. This  
466 work was supported by grant from The Asociación Española Contra el Cáncer (División  
467 provincial de Albacete). C.R-C. was investigator of the Programa Ramon y Cajal from  
468 the MEC. ADAO association for her unconditional help and support.

#### 469 **BIBLIOGRAPHY**

- 470
- 471 1. Hulka BS, Moorman PG. Breast cancer: hormones and other risk factors. *Maturitas*  
472 [Internet]. [cited 2018 Sep 5]; 61: 203–13; discussion 213. Available from  
473 <http://www.ncbi.nlm.nih.gov/pubmed/19434892>
  - 474 2. Ferlay J, Forman D, Mathers CD, Bray F. Breast and cervical cancer in 187  
475 countries between 1980 and 2010. *Lancet (London, England)* [Internet]. 2012 [cited  
476 2018 Sep 5]; 379: 1390–1. doi: 10.1016/S0140-6736(12)60595-9.
  - 477 3. Mariotto AB, Zou Z, Zhang F, Howlader N, Kurian AW, Etzioni R. Can We Use  
478 Survival Data from Cancer Registries to Learn about Disease Recurrence? The  
479 Case of Breast Cancer. *Cancer Epidemiol Biomarkers Prev* [Internet]. American  
480 Association for Cancer Research; 2018 [cited 2018 Oct 22]; . doi: 10.1158/1055-  
481 9965.EPI-17-1129.
  - 482 4. Ma L, Liu T, Jin Y, Wei J, Yang Y, Zhang H. ABCG2 is required for self-renewal and  
483 chemoresistance of CD133-positive human colorectal cancer cells. *Tumour Biol*  
484 [Internet]. 2016 [cited 2018 Oct 22]; 37: 12889–96. doi: 10.1007/s13277-016-5209-5.
  - 485 5. Liu C, Liu L, Chen X, Cheng J, Zhang H, Shen J, Shan J, Xu Y, Yang Z, Lai M, Qian  
486 C. Sox9 regulates self-renewal and tumorigenicity by promoting symmetrical cell  
487 division of cancer stem cells in hepatocellular carcinoma. *Hepatology* [Internet].  
488 2016 [cited 2018 Oct 22]; 64: 117–29. doi: 10.1002/hep.28509.
  - 489 6. Moore N, Houghton J, Lyle S. Slow-Cycling Therapy-Resistant Cancer Cells. *Stem*  
490 *Cells Dev* [Internet]. 2012 [cited 2017 Mar 7]; 21: 1822–30. doi:  
491 10.1089/scd.2011.0477.
  - 492 7. Srinivasan T, Walters J, Bu P, Than EB, Tung K-L, Chen K-Y, Panarelli N, Milsom J,  
493 Augenlicht L, Lipkin SM, Shen X. NOTCH Signaling Regulates Asymmetric Cell Fate  
494 of Fast- and Slow-Cycling Colon Cancer-Initiating Cells. *Cancer Res* [Internet]. 2016  
495 [cited 2018 Nov 5]; 76: 3411–21. doi: 10.1158/0008-5472.CAN-15-3198.
  - 496 8. Sánchez-Danés A, Larsimont J-C, Liagre M, Muñoz-Couselo E, Lapouge G,  
497 Brisebarre A, Dubois C, Suppa M, Sukumaran V, del Marmol V, Tabernero J,  
498 Blanpain C. A slow-cycling LGR5 tumour population mediates basal cell carcinoma  
499 relapse after therapy. *Nature* [Internet]. 2018 [cited 2018 Nov 5]; 562: 434–8. doi:  
500 10.1038/s41586-018-0603-3.
  - 501 9. Ramírez-Castillejo C, Sánchez-Sánchez F, Andreu-Agulló C, Ferrón SR, Aroca-  
502 Aguilar JD, Sánchez P, Mira H, Escribano J, Fariñas I. Pigment epithelium-derived  
503 factor is a niche signal for neural stem cell renewal. *Nat Neurosci* [Internet]. 2006  
504 [cited 2017 Oct 5]; 9: 331–9. doi: 10.1038/nn1657.

- 505 10. Castro-Garcia P, Díaz-Moreno M, Gil-Gas C, Fernández-Gómez FJ, Honrubia-  
506 Gómez P, Álvarez-Simón CB, Sánchez-Sánchez F, Cano JCC, Almeida F, Blanco  
507 V, Jordán J, Mira H, Ramírez-Castillejo C. Defects in subventricular zone pigmented  
508 epithelium-derived factor niche signaling in the senescence-accelerated mouse  
509 prone-8. *FASEB J* [Internet]. 2015 [cited 2017 Oct 5]; 29: 1480–92. doi:  
510 10.1096/fj.13-244442.
- 511 11. Harries RL, Owen S, Ruge F, Morgan M, Li J, Zhang Z, Harding KG, Torkington J,  
512 Jiang WG, Cai J. Impact of pigment epithelium-derived factor on colorectal cancer in  
513 vitro and in vivo. *Oncotarget* [Internet]. 2018 [cited 2018 Nov 5]; 9: 19192–202. doi:  
514 10.18632/oncotarget.24953.
- 515 12. Weidle UH, Birzele F, Tiefenthaler G. Potential of Protein-based Anti-metastatic  
516 Therapy with Serpins and Inter  $\alpha$ -Trypsin Inhibitors. *Cancer Genomics Proteomics*  
517 [Internet]. 2018 [cited 2018 Nov 5]; 15: 225–38. doi: 10.21873/cgp.20081.
- 518 13. Belkacemi L, Zhang SX. Anti-tumor effects of pigment epithelium-derived factor  
519 (PEDF): implication for cancer therapy. A mini-review. *J Exp Clin Cancer Res*  
520 [Internet]. 2016 [cited 2018 Nov 5]; 35: 4. doi: 10.1186/s13046-015-0278-7.
- 521 14. Andreu-Agulló C, Morante-Redolat JM, Delgado AC, Fariñas I. Vascular niche factor  
522 PEDF modulates Notch-dependent stemness in the adult subependymal zone. *Nat*  
523 *Neurosci* [Internet]. 2009 [cited 2017 Oct 6]; 12: 1514–23. doi: 10.1038/nn.2437.
- 524 15. Pumiglia K, Temple S. PEDF: bridging neurovascular interactions in the stem cell  
525 niche. *Nat Neurosci* [Internet]. 2006 [cited 2017 Oct 17]; 9: 299–300. doi:  
526 10.1038/nn0306-299.
- 527 16. Herpel E, Jensen K, Muley T, Warth A, Schnabel PA, Meister M, Herth FJF,  
528 Dienemann H, Thomas M, Gottschling S. The cancer stem cell antigens CD133,  
529 BCRP1/ABCG2 and CD117/c-KIT are not associated with prognosis in resected  
530 early-stage non-small cell lung cancer. *Anticancer Res* [Internet]. 2011 [cited 2018  
531 Nov 5]; 31: 4491–500. Available from  
532 <http://www.ncbi.nlm.nih.gov/pubmed/22199321>
- 533 17. Hu J, Li J, Yue X, Wang J, Liu J, Sun L, Kong D. Expression of the cancer stem cell  
534 markers ABCG2 and OCT-4 in right-sided colon cancer predicts recurrence and  
535 poor outcomes. *Oncotarget* [Internet]. 2017 [cited 2018 Nov 5]; 8: 28463–70. doi:  
536 10.18632/oncotarget.15307.
- 537 18. Nicolazzo C, Raimondi C, Francescangeli F, Ceccarelli S, Trenta P, Magri V,  
538 Marchese C, Zeuner A, Gradilone A, Gazzaniga P. EpCAM-Expressing Circulating  
539 Tumor Cells in Colorectal Cancer. *Int J Biol Markers* [Internet]. 2017 [cited 2018 Nov  
540 5]; 32: 415–20. doi: 10.5301/ijbm.5000284.
- 541 19. Xiang D, Shigdar S, Bean AG, Bruce M, Yang W, Mathesh M, Wang T, Yin W, Tran  
542 PH-L, Shamaileh H AI, Barrero RA, Zhang P-Z, Li Y, et al. Transforming doxorubicin  
543 into a cancer stem cell killer via EpCAM aptamer-mediated delivery. *Theranostics*  
544 [Internet]. 2017 [cited 2018 Nov 5]; 7: 4071–86. doi: 10.7150/thno.20168.
- 545 20. Ying X, Wu J, Meng X, Zuo Y, Xia Q, Chen J, Feng Y, Liu R, Li L, Huang W. AC133  
546 expression associated with poor prognosis in stage II colorectal cancer. *Med Oncol*  
547 [Internet]. 2013 [cited 2018 Jan 20]; 30: 356. doi: 10.1007/s12032-012-0356-z.
- 548 21. Lang J, Lan X, Liu Y, Jin X, Wu T, Sun X, Wen Q, An R. Targeting cancer stem cells  
549 with an 131I-labeled anti-AC133 monoclonal antibody in human colorectal cancer  
550 xenografts. *Nucl Med Biol* [Internet]. 2015 [cited 2018 Jan 20]; 42: 505–12. doi:  
551 10.1016/j.nucmedbio.2015.01.003.
- 552 22. Barrantes-Freer A, Renovanz M, Eich M, Braukmann A, Sprang B, Spirin P, Pardo  
553 LA, Giese A, Kim EL. CD133 Expression Is Not Synonymous to Immunoreactivity for  
554 AC133 and Fluctuates throughout the Cell Cycle in Glioma Stem-Like Cells.  
555 Harrison JK, editor. *PLoS One* [Internet]. 2015 [cited 2018 Jan 20]; 10: e0130519.  
556 doi: 10.1371/journal.pone.0130519.

- 557 23. Bourseau-Guilmain E, Béjaud J, Griveau A, Lautram N, Hindré F, Weyland M,  
558 Benoit JP, Garcion E. Development and characterization of immuno-nanocarriers  
559 targeting the cancer stem cell marker AC133. *Int J Pharm* [Internet]. 2012 [cited  
560 2018 Jan 20]; 423: 93–101. doi: 10.1016/j.ijpharm.2011.06.001.
- 561 24. Cao Z, Livas T, Kyprianou N. Anoikis and EMT: Lethal &quot;Liaisons&quot; during  
562 Cancer Progression. *Crit Rev Oncog* [Internet]. 2016 [cited 2018 Nov 5]; 21: 155–68.  
563 doi: 10.1615/CritRevOncog.2016016955.
- 564 25. Daniela da Silva S, Xu B, Maschietto M, Marchi FA, Alkailani MI, Bijjan K, Xiao D,  
565 Alaoui-Jamali MA. TRAF2 COOPERATES WITH FOCAL ADHESION SIGNALING  
566 TO REGULATE CANCER CELL SUSCEPTIBILITY TO ANOIKIS. *Mol Cancer Ther*  
567 [Internet]. 2018 [cited 2018 Nov 5]; : molcanther.1261.2017. doi: 10.1158/1535-  
568 7163.MCT-17-1261.
- 569 26. Saharat K, Lirdprapamongkol K, Chokchaichamnankit D, Srisomsap C, Svasti J,  
570 Paricharttanakul NM. Tumor Susceptibility Gene 101 Mediates Anoikis Resistance of  
571 Metastatic Thyroid Cancer Cells. *Cancer Genomics Proteomics* [Internet]. 2018  
572 [cited 2018 Nov 5]; 15: 473–83. doi: 10.21873/cgp.20106.
- 573 27. Du S, Miao J, Zhu Z, Xu E, Shi L, Ai S, Wang F, Kang X, Chen H, Lu X, Guan W,  
574 Xia X. NADPH oxidase 4 regulates anoikis resistance of gastric cancer cells through  
575 the generation of reactive oxygen species and the induction of EGFR. *Cell Death Dis*  
576 [Internet]. 2018 [cited 2018 Nov 5]; 9: 948. doi: 10.1038/s41419-018-0953-7.
- 577 28. Paoli P, Giannoni E, Chiarugi P. Anoikis molecular pathways and its role in cancer  
578 progression. *Biochim Biophys Acta* [Internet]. 2013 [cited 2018 Sep 5]; 1833: 3481–  
579 98. doi: 10.1016/j.bbamcr.2013.06.026.
- 580 29. Gilmore AP. Anoikis. *Cell Death Differ* [Internet]. 2005 [cited 2018 Sep 5]; 12 Suppl  
581 2: 1473–7. doi: 10.1038/sj.cdd.4401723.
- 582 30. Honrubia-Gómez P, López-Garrido M-P, Gil-Gas C, Sánchez-Sánchez J, Alvarez-  
583 Simon C, Cuenca-Escalona J, Perez AF, Arias E, Moreno R, Sánchez-Sánchez F,  
584 Ramirez-Castillejo C. Pedf derived peptides affect colorectal cancer cell lines  
585 resistance and tumour re-growth capacity. *Oncotarget*. 2019; 10: 2973–86. doi:  
586 10.18632/oncotarget.26085.
- 587 31. García Bueno JM, Ocaña A, Castro-García P, Gil Gas C, Sánchez-Sánchez F,  
588 Poblet E, Serrano R, Calero R, Ramírez-Castillejo C. An update on the biology of  
589 cancer stem cells in breast cancer. *Clin Transl Oncol* [Internet]. 2008 [cited 2017 Oct  
590 5]; 10: 786–93. doi: 10.1007/s12094-008-0291-9.
- 591 32. Sánchez-Sánchez F, Aroca-Aguilar J-D, Segura I, Ramírez-Castillejo C, Riese HH,  
592 Coca-Prados M, Escribano J. Expression and purification of functional recombinant  
593 human pigment epithelium-derived factor (PEDF) secreted by the yeast *Pichia*  
594 *pastoris*. *J Biotechnol* [Internet]. 2008 [cited 2017 Oct 5]; 134: 193–201. doi:  
595 10.1016/j.jbiotec.2008.01.005.
- 596 33. Franco-Chuaire ML, Ramírez-Clavijo S, Chuaire-Noack L. Pigment epithelium-  
597 derived factor: clinical significance in estrogen-dependent tissues and its potential in  
598 cancer therapy. *Iran J Basic Med Sci* [Internet]. 2015 [cited 2018 Jul 24]; 18: 837–  
599 55. Available from <http://www.ncbi.nlm.nih.gov/pubmed/26523216>
- 600 34. Martin TA, Jiang WG. Evaluation of the expression of stem cell markers in human  
601 breast cancer reveals a correlation with clinical progression and metastatic disease  
602 in ductal carcinoma. *Oncol Rep* [Internet]. 2014 [cited 2018 Mar 25]; 31: 262–72. doi:  
603 10.3892/or.2013.2813.
- 604 35. Liu S, Cong Y, Wang D, Sun Y, Deng L, Liu Y, Martin-Trevino R, Shang L,  
605 McDermott SP, Landis MD, Hong S, Adams A, D'Angelo R, et al. Breast cancer  
606 stem cells transition between epithelial and mesenchymal states reflective of their  
607 normal counterparts. *Stem cell reports* [Internet]. 2014 [cited 2018 Mar 25]; 2: 78–  
608 91. doi: 10.1016/j.stemcr.2013.11.009.

- 609 36. Moghbeli M, Moghbeli F, Forghanifard MM ahd., Abbaszadegan MR ez. Cancer  
610 stem cell detection and isolation. *Med Oncol* [Internet]. Springer US; 2014 [cited  
611 2018 Mar 25]; 31: 69. doi: 10.1007/s12032-014-0069-6.
- 612 37. Castro-Garcia P., Gil-Gas C., Honrubia-Gómez P., Alvarez-Simón C.B., Ferré-  
613 Fernández J.J., Sánchez-Sánchez F., Sánchez-Sánchez J.L., Garcia-Bueno J.M.,  
614 Sabater S., Aparicio G., Antón-Aparicio L.M. and Ramirez-Castillejo C. C-Terminal-  
615 PEDF Reduces IC50 Doses and Chemoresistant Population of CD133 and BCRP1-  
616 Positive Cancer Stem Like Cells. *J Anal Oncol* [Internet]. 2013 [cited 2017 Dec 6]; 2:  
617 195–208. doi: 10.6000/1927-7229.2013.02.04.2.
- 618 38. Yin J, Park G, Kim TH, Hong JH, Kim Y-J, Jin X, Kang S, Jung J-E, Kim J-Y, Yun H,  
619 Lee JE, Kim M, Chung J, et al. Pigment Epithelium-Derived Factor (PEDF)  
620 Expression Induced by EGFRvIII Promotes Self-renewal and Tumor Progression of  
621 Glioma Stem Cells. Hynes N, editor. *PLoS Biol* [Internet]. 2015 [cited 2017 Dec 5];  
622 13: e1002152. doi: 10.1371/journal.pbio.1002152.
- 623 39. Kondo T, Setoguchi T, Taga T. Persistence of a small subpopulation of cancer stem-  
624 like cells in the C6 glioma cell line. *Proc Natl Acad Sci U S A* [Internet]. 2004 [cited  
625 2018 Mar 25]; 101: 781–6. doi: 10.1073/pnas.0307618100.
- 626 40. Setoguchi T, Taga T, Kondo T. Cancer stem cells persist in many cancer cell lines.  
627 *Cell Cycle* [Internet]. 2004 [cited 2018 Mar 25]; 3: 414–5. doi: 10.4161/cc.3.4.799.
- 628 41. Murase M, Kano M, Tsukahara T, Takahashi A, Torigoe T, Kawaguchi S, Kimura S,  
629 Wada T, Uchihashi Y, Kondo T, Yamashita T, Sato N. Side population cells have the  
630 characteristics of cancer stem-like cells/cancer-initiating cells in bone sarcomas. *Br J*  
631 *Cancer* [Internet]. 2009 [cited 2018 Mar 25]; 101: 1425–32. doi:  
632 10.1038/sj.bjc.6605330.
- 633 42. Sun Y, Wang Y, Fan C, Gao P, Wang X, Wei G, Wei J. Estrogen promotes  
634 stemness and invasiveness of ER-positive breast cancer cells through Gli1  
635 activation. *Mol Cancer* [Internet]. 2014 [cited 2017 Jan 12]; 13: 137. doi:  
636 10.1186/1476-4598-13-137.
- 637 43. Huang W-C, Hung C-M, Wei C-T, Chen T-M, Chien P-H, Pan H-L, Lin Y-M, Chen Y-  
638 J. Interleukin-6 expression contributes to lapatinib resistance through maintenance  
639 of stemness property in HER2-positive breast cancer cells. *Oncotarget* [Internet].  
640 2016 [cited 2017 Jan 12]; 7: 62352–63. doi: 10.18632/oncotarget.11471.
- 641 44. Fiegl M, Kaufmann H, Zojer N, Schuster R, Wiener H, Müllauer L, Roka S, Huber H,  
642 Drach J. Malignant cell detection by fluorescence in situ hybridization (FISH) in  
643 effusions from patients with carcinoma. *Hum Pathol* [Internet]. 2000 [cited 2017 Jan  
644 12]; 31: 448–55. Available from <http://www.ncbi.nlm.nih.gov/pubmed/10821492>
- 645 45. Fiegl M, Massoner A, Haun M, Sturm W, Kaufmann H, Hack R, Krugmann J, Fritzer-  
646 Szekeres M, Grünewald K, Gastl G, Grünewald K, Gastl G. Sensitive detection of  
647 tumour cells in effusions by combining cytology and fluorescence in situ  
648 hybridisation (FISH). *Br J Cancer* [Internet]. 2004 [cited 2017 Jan 12]; 91: 558–63.  
649 doi: 10.1038/sj.bjc.6601942.
- 650 46. Frisch SM, Francis H. Disruption of epithelial cell-matrix interactions induces  
651 apoptosis. *J Cell Biol* [Internet]. 1994 [cited 2018 Mar 25]; 124: 619–26. Available  
652 from <http://www.ncbi.nlm.nih.gov/pubmed/8106557>
- 653 47. Ohmura-Kakutani H, Akiyama K, Maishi N, Ohga N, Hida Y, Kawamoto T, Iida J,  
654 Shindoh M, Tsuchiya K, Shinohara N, Hida K. Identification of Tumor Endothelial  
655 Cells with High Aldehyde Dehydrogenase Activity and a Highly Angiogenic  
656 Phenotype. Morishita R, editor. *PLoS One* [Internet]. 2014 [cited 2018 Mar 25]; 9:  
657 e113910. doi: 10.1371/journal.pone.0113910.

## 658 FIGURE LEGENDS

659 **Figure 1. LT+ population display cancer stem cells characteristics.** (A) Cells were  
660 stained with DDAO and cultivated 8DIV in monolayer or as mammospheres. Both cell  
661 lines showed LT+ population and it was higher in mammosphere assays (cytometry  
662 assay). Quantification of LT+ cells (n=3) is shown. (B) Growing patterns of LT+ and  
663 LT- cells. Pa00 cells were stained, grown 8DIV (400cells/well) and then sorted  
664 according to their DDAO content. It was checked the number of living cells after 3DIV  
665 by methyl purple assay. LT- cells grew similar to control and faster than LT+ cells. (C)  
666 Docetaxel dose-response curves for LT+, LT- and control cells. Cells were stained  
667 with DDAO and grown for 8DIV, sorted by their content of DDAO and grown with  
668 increasing concentration of docetaxel. LT+ cells showed more resistance against  
669 docetaxel than LT-. (D) 5000 cells were injected in nude mice in each case. The  
670 volume of the tumour is similar when injecting LT- cells and control non-separated  
671 cells but smaller when injecting LT+ cells. All tumours were palpable at the same time.  
672 LT+ tumours grew slowly compared to control or LT- group. (E) Pa00 LT- cells failed  
673 to form tumours when injected in a small amount of cells. All set of tumour cells were  
674 able to form tumours when 5 000 cells were injected. However, LT- cells displayed a  
675 less frequency in tumour forming when 1 200 or 350 000 cells were injected.

676 **Fig 2. Pigmental Epithelium Derived Factor (PEDF) increases the number of LT+ cells**  
677 **and the Docetaxel resistance of breast cancer cells.** (A) Cells treated with chronic  
678 PEDF showed a different morphology than control. (B) Quantification of morphology  
679 differences induced by PEDF treatment. (C) Growing pattern n=3 after 3DIV of PEDF  
680 treated cells and control. PEDF chronic treated cells grew slower than control. (D)  
681 Docetaxel dose-response curve of PEDF treated cells and control, n=3. PEDF chronic  
682 treated cells were more resistant against Docetaxel. (E) PEDF chronic treatment  
683 increased the number of LT+ cells in vitro (n=3). (F) Docetaxel dose-response curve  
684 of LT+ PEDF treated cells and LT+ cells, n=3. LT+ PEDF chronic treated cells were

685 more resistant against Docetaxel than LT+. (G) PEDF treated cells and control cells  
686 were injected into nude mice. PEDF chronic treated cells grew slower than control. (H)  
687 Histology of PEDF treated tumours and control tumours. Necrotic areas are bigger in  
688 control compared to PEDF treatment.

689 **Fig 3. CTE-PEDF induces anoikis in vivo and reduces resistance against Docetaxel**  
690 **without affecting LT+ population.** (A) CTE-PEDF construction (B) Pa00 cells were  
691 treated chronically with CTE (200ng/uL). After a week they showed an increase in  
692 anoikis. (C) Quantification of CTE induced morphology. (D) Growing pattern n=3 after  
693 3DIV of CTE treated cells and control. CTE chronic treated cells grew slower than  
694 control. (E) Docetaxel dose-response curve of CTE treated cells and control, n=3.  
695 CTE chronic treated cells were less resistant against Docetaxel.

696 **Fig 4. Cter-PEDF and CTE-PEDF treatments decrease CSC in vivo in Pa00 ascitis cell**  
697 **line.** (A) 5000 Pa00 cells were injected in matrigel with 200ng/uL of Cter-PEDF, CTE-  
698 PEDF or PBS (control). A cytometry assay showed that the number of CSC is lower  
699 in both treatments compared to control. (B) Quantification of positive cells in each  
700 treatment compared to control (n=3). Significant differences are shown.

# Figures

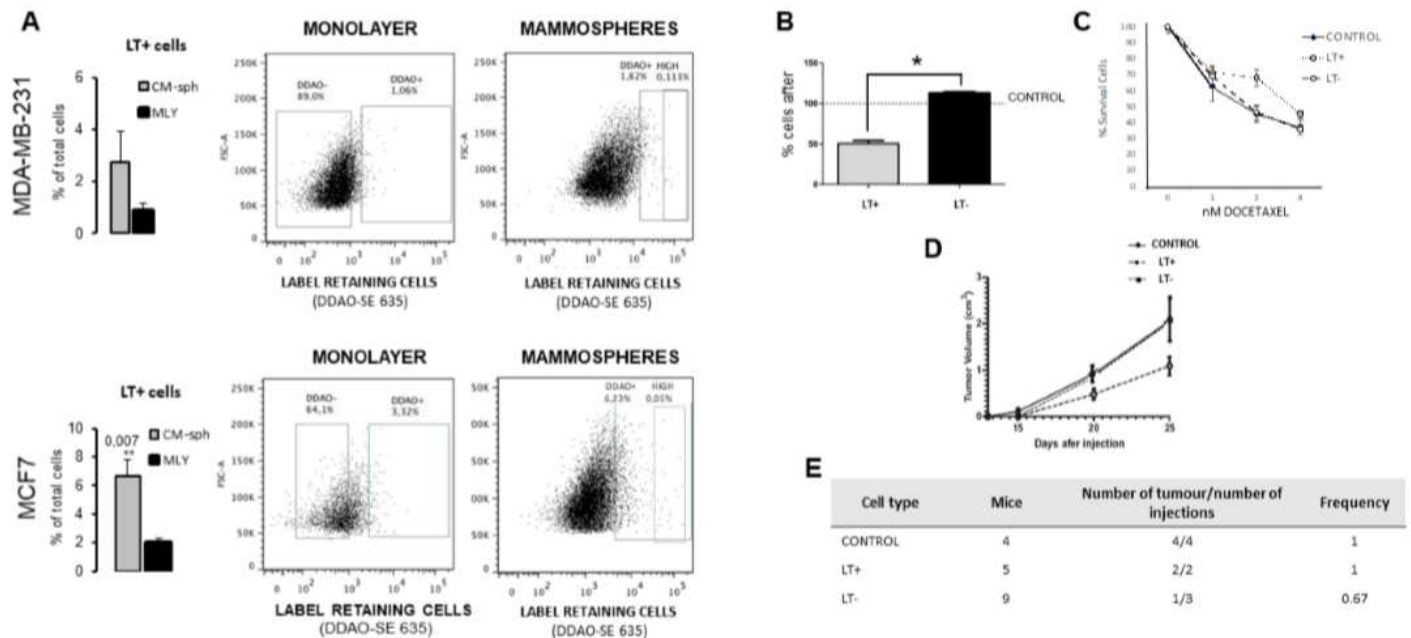


**Figure 1**

LT+ population display cancer stem cells characteristics. (A) Cells were stained with DDAO and cultivated 8DIV in monolayer or as mammospheres. Both cell lines showed LT+ population and it was higher in mammosphere assays (cytometry assay). Quantification of LT+ cells (n=3) is shown. (B) Growing patterns of LT+ and LT- cells. Pa00 cells were stained, grown 8DIV (400cells/well) and then sorted according to their DDAO content. It was checked the number of living cells after 3DIV by methyl purple assay. LT- cells grew similar to control and faster than LT+ cells. (C) Docetaxel dose-response curves for LT+, LT- and control cells. Cells were stained with DDAO and grown for 8DIV, sorted by their content of DDAO and grown with increasing concentration of docetaxel. LT+ cells showed more resistance against docetaxel than LT-. (D) 5000 cells were injected in nude mice in each case. The volume of the tumour is similar when injecting LT- cells and control non-separated cells but smaller when injecting LT+ cells. All tumours were palpable at the same time. LT+ tumours grew slowly compared to control or LT- group. (E) Pa00 LT- cells failed to form tumours when injected in a small amount of cells. All set of tumour cells were able to form tumours when 5 000 cells were injected. However, LT- cells displayed a less frequency in tumour forming when 1 200 or 350 000 cells were injected.

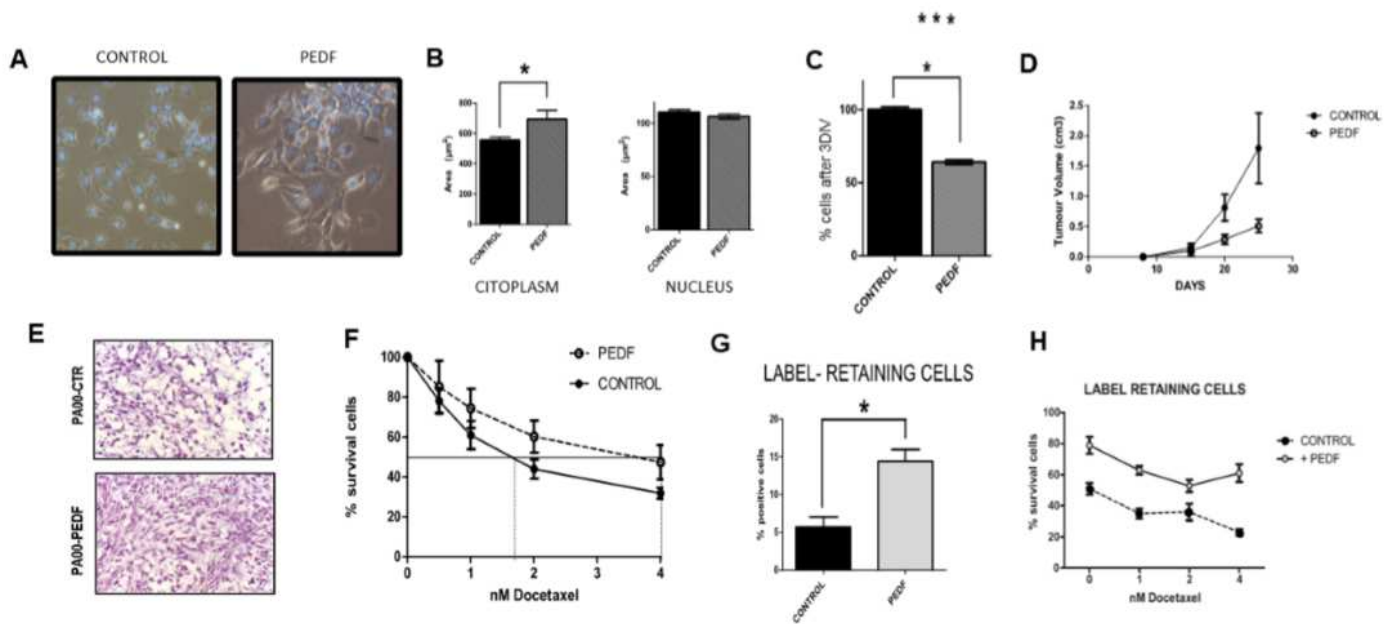


**Figure 2**

Pigmental Epithelium Derived Factor (PEDF) increases the number of LT+ cells and the Docetaxel resistance of breast cancer cells. (A) Cells treated with chronic PEDF showed a different morphology than control. (B) Quantification of morphology differences induced by PEDF treatment. (C) Growing pattern  $n=3$  after 3DIV of PEDF treated cells and control. PEDF chronic treated cells grew slower than control. (D) Docetaxel dose-response curve of PEDF treated cells and control,  $n=3$ . PEDF chronic treated cells were more resistant against Docetaxel. (E) PEDF chronic treatment increased the number of LT+ cells in vitro ( $n=3$ ). (F) Docetaxel dose-response curve 683 of LT+ PEDF treated cells and LT+ cells,  $n=3$ . LT+ PEDF chronic treated cells were more resistant against Docetaxel than LT+. (G) PEDF treated cells and control cells were injected into nude mice. PEDF chronic treated cells grew slower than control. (H) Histology of PEDF treated tumours and control tumours. Necrotic areas are bigger in control compared to PEDF treatment.

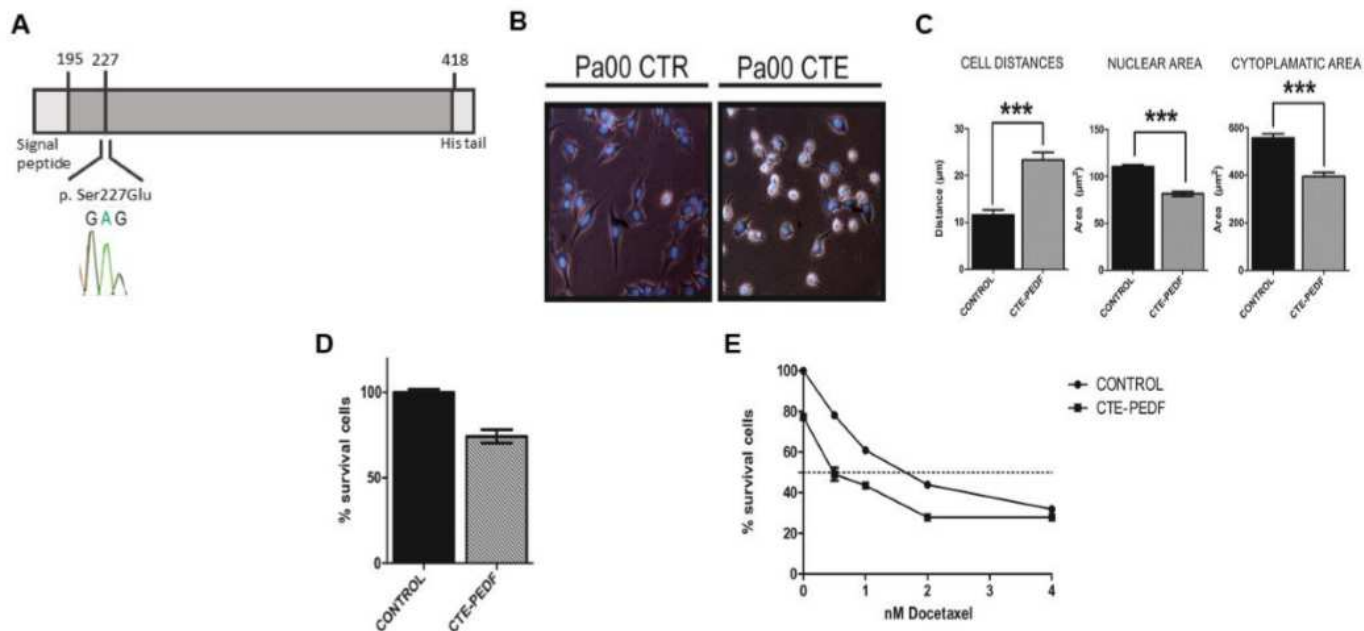


**Figure 3**

CTE-PEDF induces anoikis in vivo and reduces resistance against Docetaxel without affecting LT+ population. (A) CTE-PEDF construction (B) Pa00 cells were treated chronically with CTE (200ng/uL). After a week they showed an increase in anoikis. (C) Quantification of CTE induced morphology. (D) Growing pattern n=3 after 3DIV of CTE treated cells and control. CTE chronic treated cells grew slower than control. (E) Docetaxel dose-response curve of CTE treated cells and control, n=3. CTE chronic treated cells were less resistant against Docetaxel.

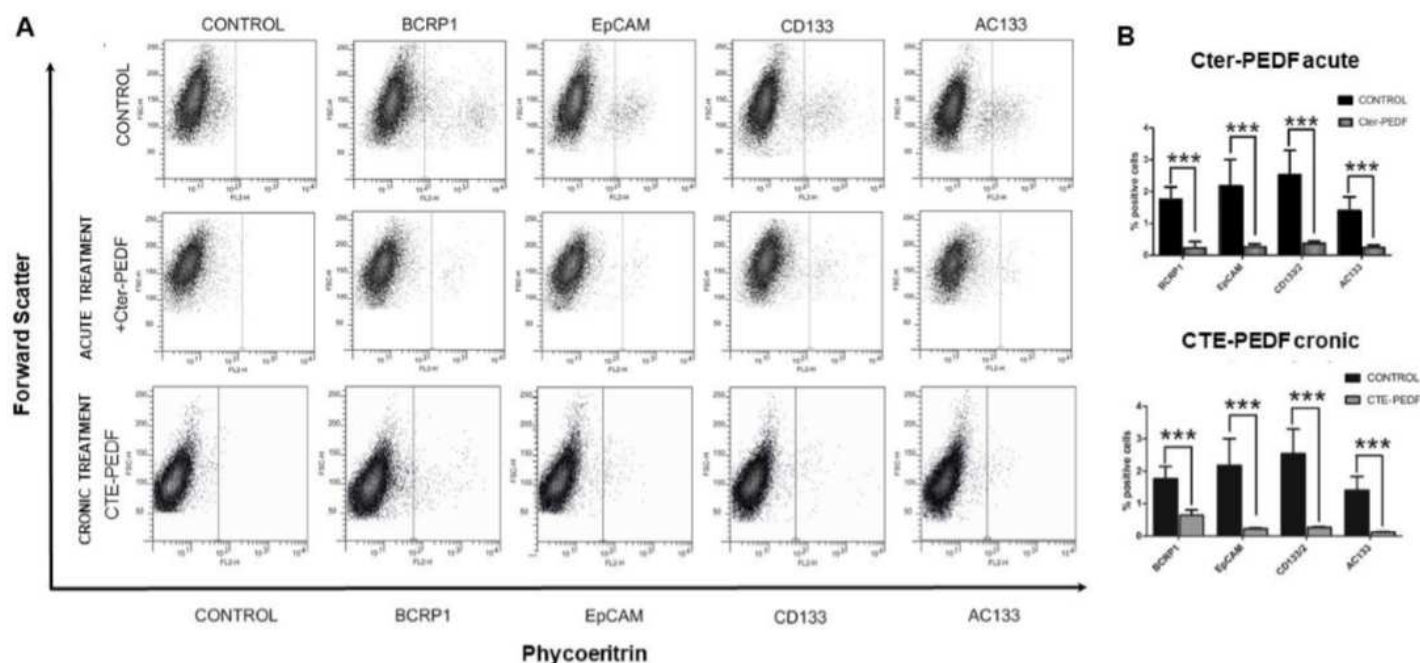


## Figure 4

Cter-PEDF and CTE-PEDF treatments decrease CSC in vivo in Pa00 ascitis cell line. (A) 5000 Pa00 cells were injected in matrigel with 200ng/uL of Cter-PEDF, CTE- PEDF or PBS (control). A cytometry assay showed that the number of CSC is lower in both treatments compared to control. (B) Quantification of positive cells in each treatment compared to control (n=3). Significant differences are shown.